Risk Analysis, Vol. 39, No. 3, 2019 DOI: 10.1111/risa.13192

A Data-Driven Approach to Assessing Supply Inadequacy Risks Due to Climate-Induced Shifts in Electricity Demand

Sayanti Mukherjee [1,*] **and Roshanak Nateghi** [2]

The U.S. electric power system is increasingly vulnerable to the adverse impacts of extreme climate events. Supply inadequacy risk can result from climate-induced shifts in electricity demand and/or damaged physical assets due to hydro-meteorological hazards and climate change. In this article, we focus on the risks associated with the unanticipated climate-induced demand shifts and propose a data-driven approach to identify risk factors that render the electricity sector vulnerable in the face of future climate variability and change. More specifically, we have leveraged advanced supervised learning theory to identify the key predictors of climate-sensitive demand in the residential, commercial, and industrial sectors. Our analysis indicates that variations in mean dew point temperature is the common major risk factor across all the three sectors. We have also conducted a statistical sensitivity analysis to assess the variability in the projected demand as a function of the key climate risk factor. We then propose the use of scenario-based heat maps as a tool to communicate the inadequacy risks to stakeholders and decisionmakers. While we use the state of Ohio as a case study, our proposed approach is equally applicable to all other states.

KEY WORDS: Climate-induced demand shifts; data-driven risk analytics; electricity adequacy planning; electricity demand–climate change nexus; sectoral demand analysis

1. INTRODUCTION

Ensuring the security and resilience of the electric grid is of utmost importance. Due to the complex interdependencies that exist between the electric power network and all other critical infrastructure systems in the United States, disruptions in the electricity sector can adversely affect our national security, digital economy, public health, and the environment, causing devastating socioeconomic impacts. The current U.S. electricity infrastructure is aging (some of which was built in 1880s) and is suffering from underinvestment (Mukherjee, 2017; Mukherjee & Hastak, 2016). Under a "business-as-usual" scenario, the electricity sector is failing to keep pace with our society's rising electricity demand (ASCE, 2017; Mukherjee & Hastak, 2016). Moreover, climate and weather extremes present a growing threat to our electric infrastructure systems (Nateghi, Guikema, Wu, & Bruss, 2016). In fact, the U.S. grid is becoming increasingly vulnerable to weather and climate-induced failures, which will likely be exacerbated in the future in absence of adequate anticipatory measures in enhancing the resilience of the electrical grid (DOE, 2016; Hines, Apt, & Talukdar, 2009; Mukherjee, 2017; Mukherjee, Nateghi, & Hastak, 2018). Extreme hydro-climatological hazards such as coastal flooding (due to sea-level rise, or shifts in precipitation patterns, and land-use change), wildfires, droughts, or heatwaves are the imminent risks that can result in infrastructure damage and/or deviated patterns in end-use demands, leading to electric power supply

[1]University at Buffalo, The State University of New York (SUNY), Buffalo, NY, USA.
[2]Purdue University, West Lafayette, IN, USA.
[*]Address correspondence to Sayanti Mukherjee, Department of Industrial and Systems Engineering, University at Buffalo (SUNY), Buffalo NY 14260; sayantim@buffalo.edu.

shortages (DOE, 2013; Mukherjee, Vineeth, & Nateghi, 2018). In this article, we focus primarily on assessing the sensitivity of end-use electricity demand to climate variability and change. Therefore, modeling damaged infrastructure due to increased frequency or disruptive force of natural disasters under climate change is outside the scope of the analysis presented in this article.

While many of the energy demand–climate nexus studies focus on projecting the aggregate demand (Crowley & Joutz, 2005; IEA, 2015; Miller, Jin, Hayhoe, & Auffhammer, 2007; Sullivan, Colman, & Kalendra, 2015), we conducted our analysis at the "sectoral" (i.e., residential, commercial and industrial) level, since the climate sensitivity of load varies substantially as a function of the type of consumers served (Mukherjee & Nateghi, 2018). Sectoral[3]-level demand management is thus extremely important for better characterizing electricity demand trends and informed design of targeted energy efficiency and conservation policy. Our model outputs can be readily integrated with energy-economy models such as MARKAL (MARKet Allocation) (Loulou, Goldstein, & Noble, 2004) and NEMS (National Energy Modeling System) (EIA, 2014b) to provide important policy information related to demand-side management, and choices of future energy supply (Nateghi & Mukherjee, 2017).

According to the North American Electricity Reliability Corporation (NERC), the performance of the electricity sector can be assessed via the *adequate level of reliability* metric. Adequate level of reliability consists of two fundamental concepts of "system adequacy" and "security/operating reliability" (NERC, 2007). *System adequacy* relates to the existence of sufficient capacity within the system to satisfy consumer load, considering the system operational constraints (Li, 2014). Load forecasting lies at the heart of system adequacy planning in the electricity sector, as shown in Fig. 1 (Hirst, 1992). Inaccurate load forecasts can result in under-/overestimation of reserve margins, leading to substantial socioeconomic losses. In this context, it is noteworthy that accurate estimates of both peak load and total electricity consumption are critical for integrated adequacy planning (NYISO, 2016). Peak demand indicates a small portion of the annual overall power usage and is a significant parameter for maintaining the reliability standards of the grid, while consumption indicates the total demand during a specific span of time (NYISO, 2016). In this article, we focus on the monthly aggregated consumption patterns to characterize the load function for the climate-sensitive portion of the demand. However, the methods used in this research can easily be extended to assess the climate sensitivity of peak load as well.

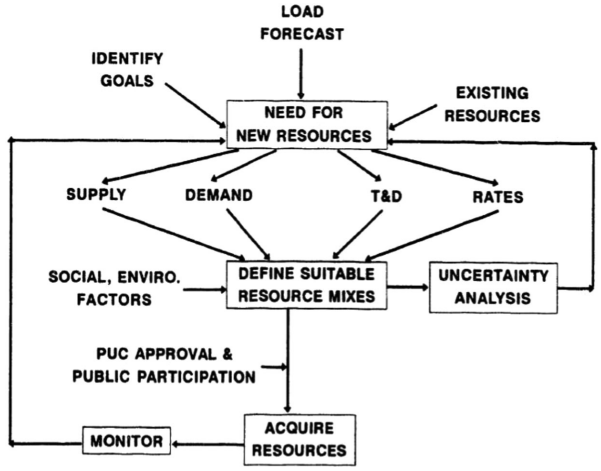

Fig. 1. Power systems load forecast and resource adequacy planning (Hirst, 1992).

While great technical advancements have been made in forecasting short-term (peak and total) load, significant knowledge gaps exist in medium- and long-term load forecasting, particularly in characterizing the climate–demand nexus. Accurate projections of medium- and long-term forecasts under climate variability and change remain as one of the key challenges for many regional transmission organizations (RTOs) in the United States. For instance, the RTO—PJM Interconnection, serving all or parts of Delaware, Illinois, Indiana, Kentucky, Maryland, Michigan, New Jersey, North Carolina, Ohio, Pennsylvania, Tennessee, Virginia, West Virginia, and the District of Columbia—has identified systematic bias in its forecasting methods and has made multiple attempts to address the bias in its estimates (PJM Interconnection, 2016). A recent report by PJM Interconnection states that its forecasts substantially underperformed, largely due to the limited flexibility and poor generalization performance of the models used (PJM Interconnection, 2016). Moreover, the existing integrated energy-economy models such as MARKAL (Loulou et al., 2004) and NEMS (EIA, 2014b) that are typically used for medium- and long-term planning and policy analysis suffer from major limitations. For instance, MARKAL

[3]The term "sectoral" indicates that the load projection is conducted for each of the individual electricity sectors.

does not allow for modeling the impact of climate variability on load projections exogenously (Nateghi & Mukherjee, 2017). On the other hand, NEMS characterizes the climate–demand nexus using aggregated (annual) temperature metrics such as heating and cooling degree days that fail to capture the temporal variability of temperature, and are inadequate measures of surface air heat content (Mukherjee & Nateghi, 2017). Therefore, NEMS underestimates the climate sensitivity of load, particularly under climate change (Mukherjee & Hastak, 2017; Mukherjee & Nateghi, 2017; Pielke, Davey, & Morgan, 2004).

Mis-characterizing the climate sensitivity of load can be very costly, since climate variability can induce *unexpected* supply shortages and cause price spikes of over 500% (as in the cases of TX in 2011 and NY in 2014), leading to outages with significant social and economic costs. Moreover, insufficient access to space conditioning during severe climate events can be lethal, such as the July 1995 heatwave in the Midwest that claimed the lives of over 700 people in Chicago. The long-term social and economic costs of not incorporating weather and climatic extremes into load forecasting and adequacy planning will even exacerbate in the future. This is because climate change will likely increase the frequency and intensity of extreme events that will further stress the nation's electric grid (Nateghi et al., 2016).

In short, the existing knowledge gaps in the medium- and long-term load forecasting can be summarized as follows: (i) not exogenously accounting for climate variability and change (e.g., MARKAL) (Loulou et al., 2004); (ii) using aggregated temperature metrics (e.g., degree day variables) as a key predictor of the climate-sensitive load, which fail to pick up seasonality and underestimate the climate sensitivity of load (Amato, Ruth, Kirshen, & Horwitz, 2005; Mirasgedis et al., 2007; Nateghi & Mukherjee, 2017; Sailor, 2001; Sailor & Muñoz, 1997); and (iii) prevalent application of models with poor generalization performance that consistently yield biased projections (PJM Interconnection, 2016). To address these gaps, we propose a rigorous, data-driven methodology to accurately characterize the climate–load nexus and facilitate improved modeling and planning in the power sector in order to minimize the inadequacy risks.

The central hypothesis guiding our analysis is that the evidently costly and yet unpredictable climate-induced load variation is rooted in the use of unsuitable climate predictors and inadequate empirical models. To test our hypothesis, we rigorously assess the performance of a wide range of statistical models that are trained with a large collection of candidate climate predictors. The statistical tests indicate that our final best predictive model can adequately characterize the climate–demand nexus in each sector. Moreover, our proposed method facilitates identifying the climate factors that most influence the end-use electricity consumption in each sector. Herein, we also illustrate how the seasonal supply inadequacy risks can be assessed by comparing the projected demand (under climate contingencies) and the planned capacity in the region of interest. To illustrate the applicability of our proposed methodology, we have selected the state of Ohio as a case study due to the following reasons:

- It is among the most energy-intensive states in the United States (Sailor & Muñoz, 1997);
- It is highly vulnerable to reduced power generation capacity due to higher temperatures (DOE, 2015); and
- It is expected to satisfy increased electricity demand for space cooling during the summer owing to projected increased levels of heat and humidity (DOE, 2015). Fig. 2 below illustrates how the state of Ohio has continued to experience above-average temperatures (NOAA, 2016a) in 2016 during the summer months.

Thus, Ohio presents an interesting case for estimating electricity inadequacy risks under climate variations.

This article is organized as follows: in Section 2, we provide a brief review of the existing literature related to electricity-sector risks and vulnerability under climate change. In Section 3, we describe the process of data collection, filtering, and preprocessing. In Section 4, we review the methodology used in this article, and present the results of our analysis in Section 5. In Section 6, we summarize the results of scenario-based sensitivity analysis of the sectoral electricity demands under various degrees of climate perturbations. Section 7 describes the use of heat-maps in communicating the inadequacy risks. We conclude the article in Section 8 by summarizing our findings and making recommendations for future research.

2. LITERATURE REVIEW

Recent studies published by the National Association of Regulatory Utility Commission (NARUC) focused on the importance of resilience

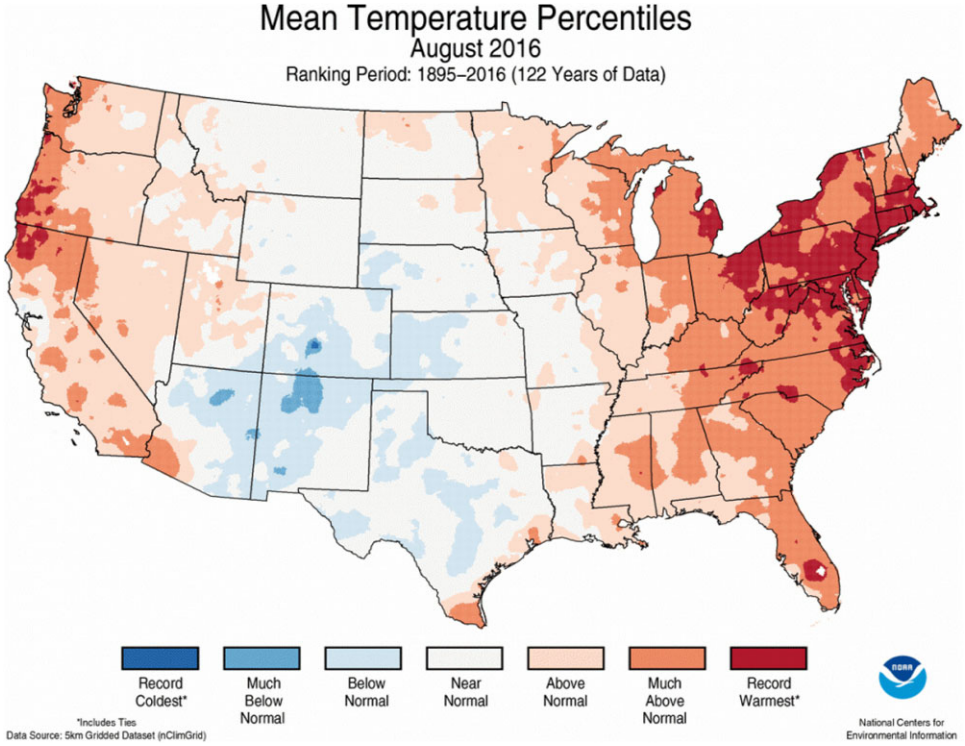

Fig. 2. Statewide average temperature ranks, January to June 2016 (Period: 1895–2016).
Source: NOAA—National Temperature and Precipitation Maps, January to June 2016 (NOAA, 2016b).

incorporation in the electricity sector for long-term benefits of the grid and the society (Keogh & Cody, 2013; Mukherjee, 2017; Mukherjee & Hastak, 2016; Stockton, 2014). Quantitative vulnerability assessment is the first key step in enhancing resilience of these systems (Birkmann, 2006; Gallopín, 2006). In the face of climate change, the electricity sector's vulnerability to higher frequency of supply shortages (due to both physical damage and climate-induced demand shifts) is increasing (Davis & Clemmer, 2014; DOE, 2016). Vulnerability assessment is thus critical for identifying efficient capacity expansion and load-modifying solutions (such as demand-response) (DOE, 2016).

Although it has been well documented that climate and weather factors play a major role in shaping the end-use demand, there is a scant body of literature assessing the sector's vulnerability to climate-driven shifts in electricity demand. A comprehensive literature review by Mideksa and Kallbekken (2010) highlighted the significant existing gaps in modeling the impact of climate change on the electricity sector. Sailor and Muñoz (1997) and Sailor (2001) assessed the state-level vulnerabilities of the electricity sector by modeling the relationships between electricity load and climate using ordinary least squares (OLS) regression method. Amato et al. (2005) estimated the energy demand–climate relationships using a two-step generalized linear model (GLM) for the Commonwealth of Massachusetts. Ruth and Lin (2006) conducted a similar study for the state of Maryland, fitting a linear regression model to characterize the climate–demand relationship. However, later analyses by Mukherjee et al. (2018) and Mukherjee and Nateghi (2017, 2018) suggested that the complex climate–demand relationship cannot be adequately captured using linear models. Moreover, most of the previous studies leveraged the conventionally used temperature metrics (aka the cooling and heating degree day variables) to relate climate variability and electricity demand (Amato et al., 2005; Mirasgedis et al., 2007; Ruth & Lin, 2006; Sailor, 2001; Sailor & Muñoz, 1997). Major issues associated with considering the degree day variables in the climate–demand models are as follows: (i) degree day estimation uses an arbitrary balance point temperature that is often inaccurate and varies across the regions (Brown, Cox, Staver, & Baer, 2014; Mukherjee & Nateghi,

2017); (ii) these variables are inadequate measures of surface heating and cooling as they do not account for the specific humidity in the atmosphere (Pielke et al., 2004); and (iii) strong anti-correlation among the cooling and heating degree days leads to biased statistical inferences (Mukherjee & Nateghi, 2017).

Furthermore, an extensive review of existing studies related to impacts of climate change on electricity systems by Chandramowli and Felder (2014) indicated that the existing integrated assessment models (IAMs) used for long-term electricity demand planning and policy formulations do not adequately consider the climate change trends as exogenous inputs in these models. Thus, the effects of climate change on the outcomes of such IAMs are confounded with uncertainties (Chandramowli & Felder, 2014). Moreover, many energy-economy models such as the NEMS (EIA, 2014b) and MARKAL (Loulou et al., 2004) also underestimate the weather- and climate-change risks.

To address these gaps, we propose a data-driven approach to capture the state-level climate–demand nexus and identify the key climate risk factors. Our proposed approach overcomes the major limitations of the existing models in the following ways: (i) our flexible, statistical model accounts for the complex relationship between climate and electricity demand, instead of assuming a linear relationship; (ii) we have considered more suitable measures of heat stress (e.g., dew point temperature) instead of the conventionally used degree day metrics (Amato et al., 2005; Kapelner & Bleich, 2013; Ruth & Lin, 2006; Sailor, 2001; Sailor & Muñoz, 1997); (iii) we have implemented a robust, data-driven variable selection technique to identify key climate risk factors—in terms of inducing the largest shift in load for each sector; and, finally, (iv) we propose a risk communication tool to visualize the risks associated with climate-driven demand shifts in each sector under different climate perturbations scenarios. Our model results can easily be integrated with the existing energy-economy models to estimate weather- and climate-induced risks to help in the policy and strategic decision making, considering deep uncertainties of the future.

3. DATA COLLECTION AND PROCESSING

We used four categories of data for our analysis, viz., (i) sectoral end-use electricity consumption, (ii) climate data, (iii) weather data, and (iv) socioeconomic data. Electricity consumption data for the state of Ohio were obtained from the U.S. Energy Information Administration (EIA) (form EIA-826) (EIA, 2017a). We used a monthly temporal scale in our analysis because daily estimates are too refined for long-term projections, while the use of annual scale hinders accurate characterization of seasonal climatic signals. The monthly sectoral electricity consumption data for the period of 1990–2015 were extracted from the database and were trend-adjusted to remove time effects such as population increase, land use change, technology, and policy change over time (Sailor & Muñoz, 1997). Monthly climate data and daily weather data from all the weather stations located across the state of Ohio were obtained from the National Climatic Data Center (NCDC) of the National Oceanic and Atmospheric Administration (NOAA) for the period of analysis. Socioeconomic data were obtained from the U.S. Department of Labor, Bureau of Labor Statistics (USDL, 2016).

We implemented our analysis for the residential, commercial, and industrial sectors. Table I provides descriptive statistics (mean, median, minimum, maximum, standard deviation, skewness, and kurtosis) of the sectoral electricity demands. The industrial sector's demand shows the least variation as opposed to the residential sector, which has the largest demand variability.

Fig. 3 provides a graphical representation (violin plot) of electricity demand in the three sectors. A violin plot is a combination of a boxplot and a kernel density plot. In other words, in a violin plot, a

Table I. Descriptive Statistics of Monthly Sectoral Electricity Demand for the State of Ohio During 1990 January to 2015 December

	Monthly Electricity Demand (GWhr/month)						
Sector	Mean	Median	Min	Max	Std. Dev.	Skewness	Kurtosis
Residential	4,012.3	3,963.7	2,780.7	5,955.9	728.9	0.39	−0.77
Commercial	3,446.3	3,399.4	2,976.3	4,552.3	291.6	0.80	0.28
Industrial	5,188.2	5,213.3	4,552.2	5,667.9	201.0	−0.40	0.11

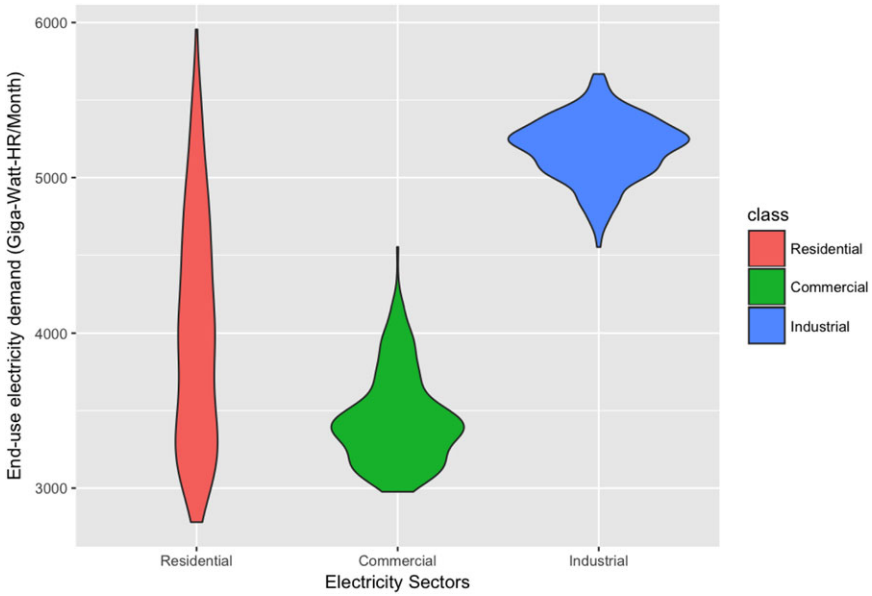

Fig. 3. Violin plots of end-use electricity demand for the three sectors of residential, commercial, and industrial.

rotated kernel density plot is added on the two sides of the boxplot (Hintze & Nelson, 1998). It can be observed that the distributions of the residential and commercial sectors' electricity demand (consumption) are right-skewed whereas that of the industrial sector is left-skewed. It can be also observed that the residential electricity demand is much more heterogeneous and long-tailed compared to the other two sectors.

4. METHODOLOGY

In this section, we provide a brief overview of the statistical learning methods used in our analysis and the procedure used to select our final model. The section begins with a brief introduction of the supervised statistical learning followed by a description of the ensemble tree-based random forest (RF) model, which was selected as our final model. We conclude this section by discussing the bias-variance tradeoff, the tradeoff between predictive accuracy and model interpretability, and the procedure for our final model selection.

4.1. Supervised Learning

Supervised learning is used in predictive modeling. It involves making inference about an unknown function f that is used to predict the response variable $\mathbf{Y}$ using a p dimensional vector of predictor variables $\mathbf{X}$. The generalized relationship can be mathematically represented as $\mathbf{Y} = f(\mathbf{X}) + e$. The objective of supervised learning is to best capture the relationship between the response and the predictor variables by minimizing a given error function that measures the deviation of observed from the estimated values of $\mathbf{Y}$. We trained our data with various parametric, semi-parametric, and nonparametric supervised learning methods. More specifically, we trained our data leveraging various statistical learning methods such as generalized linear model (GLM) (Guikema & Coffelt, 2008; Nelder & Wedderburn, 1972), generalized additive model (GAM) (Guikema & Coffelt, 2008; Hastie & Tibshirani, 1990; Hastie & Tibshirani, 1986), multivariate adaptive regression splines (MARS) (Friedman, 1991; Guikema & Coffelt, 2008), and random forest (RF) (Breiman, 2001; Hastie, Tibshirani, & Friedman, 2003). A brief overview of the RF method is provided below since it was found to best capture the energy demand–climate nexus and was selected as our final model to estimate the supply inadequacy risks due to climate-induced shifts in electricity demand. However, details on methodological backgrounds of the other models such as GLM, GAM, and MARS can be found in the Appendix of this article.

4.1.1. Random Forest (RF)

RF is a nonparametric tree-based ensemble data-miner (Breiman, 2001). The method consists of B bootstrapped regression trees (T_b). In general, single regression trees are low-bias, high-variance techniques. In other words, they can capture the structure of the data really well (low bias), but are highly sensitive to outliers (high variance) (James, Witten, Hastie, & Tibshirani, 2013). RF overcomes the issue of high variance by leveraging model averaging as a variance reduction technique. The final estimate of a RF method is the average of predictions across all trees:

$$\hat{f}_{rf}^{B}(x) = \frac{1}{B}\sum_{b=1}^{B} T_b(x).$$

The algorithm for developing a RF model in a regression setting is as follows:

(i) Create a training set by selecting N bootstrap resamples of the data; treat the remaining data as the validation set to estimate the tree's prediction error.
(ii) Fit a regression tree to the training data set by randomly selecting predefined "m" ($\ll M$) variables to split on; here, M represents the total number of covariates used in the model.
(iii) Choose the optimal splitting values using the "m" allowable splitting variables, growing the tree to completion.
(iv) Test the predictive error with the remaining data.
(v) Repeat steps (i) to (iv) for K (a predefined value) number of times to develop K trees. The number of trees is selected such that the out-of-sample errors are minimized. Final predictions are given by the unweighted average of the predictions of the K regression trees.

The advantage of this method is that it can capture the nonlinear structure of data very well and is robust to outliers and noise (Hastie et al., 2003). It also generally offers a strong predictive accuracy (Hastie et al., 2003). The method is also simple to implement and does not require arduous fine-tuning of the parameters. For model inference, a RF model provides a list of important variables by ranking them in terms of their contribution to the out-of-sample predictive accuracy (Hastie, Tibshirani, & Friedman, 2008).

4.2. Predictive Accuracy Versus Model Interpretability

Flexible nonparametric methods generally better capture the variation in data and have higher predictive power than the more "restrictive" parametric models. However, improved predictive power often comes at the cost of ease of interpretability. To make inferences based on nonparametric models such as the method of RF, *partial dependence plots (PDPs)* can be used. PDPs help in understanding the effects of the predictor variable of interest x_j on the response in a "ceteris paribus" condition (i.e., controlling for all the other predictors). Mathematically, the estimated PDP can be represented as (Kapelner & Bleich, 2013):

$$\widehat{f}_j(x_j) = 1/n \sum_{i=1}^{n} \widehat{f}_j(x_j, x_{-j,i}).$$

Here, $\hat{f}$ denotes the statistical model; n denotes the number of observations in the training data set; x_{-j} denotes all the variables except x_j. The estimated PDP of the predictor x_j provides the average value of the function $\hat{f}$ when x_j is fixed and x_{-j} varies over its marginal distribution.

4.3. Bias Variance Tradeoff

Toachieve optimal generalization performance for a statistical model, its complexity should be controlled through bias-variance trade off. Cross-validation is the most widely used technique for balancing models' bias and variance. In this study, we used a randomized holdout analysis to estimate the predictive accuracy of the models. More specifically, out-of-sample predictive accuracy of each model was calculated by implementing 30-fold random holdout validation tests where in each iteration, 10% of the data was randomly held out and the model was trained with the remaining data, and tested using the held-out sample.

4.4. Model Selection

We developed all the models as described above and then selected the final best model using the following sequential process:

(i) Separate statistical models for each sector were developed, using all the available predictor variables, and both the in-sample fit and

Table II. Comparative Analysis of Model Performance for Model Selection

				In-Sample		Out-of-Sample	
Sector	#	Model	R^2	RMSE	MAE	RMSE	MAE
Residential	1	Mean-only	NA	725.23	609.96	715.83	596.35
	2	GLM	0.499	513.28	414.92	532.15	429.95
	3	GAM	0.892	220.94	175.44	255.84	207.45
	4	MARS	0.929	198.53	160.09	273.5	218.97
	5	RF	0.976	112.39	84.90	271.27	212.08
Commercial	1	Mean-only	NA	291.58	228.51	289.49	225.96
	2	GLM	0.662	169.51	136.53	187.85	150.45
	3	GAM	0.885	89.73	72.68	114.45	94.75
	4	MARS	0.887	97.63	72.68	113.34	91.94
	5	RF	0.975	45.89	36.25	110.05	89.08
Industrial	1	Mean-only	NA	291.13	228.02	199.05	159.61
	2	GLM	0.262	172.46	136.09	186.65	148.67
	3	GAM	0.239	164.70	128.33	186.01	146.46
	4	MARS	0.205	164.70	128.33	177.90	141.36
	5	RF	0.876	70.64	54.06	167.18	130.39

out-of-sample predictive accuracy of the models were estimated.

(ii) The model that outperformed all other models, in terms of both in-sample fit and out-of-sample prediction accuracy, was then selected.

(iii) Per Occam's razor principle of selecting the simplest model that best captures the variation in data, we applied a data-driven variable reduction technique to reduce the input data and identify the key variables that contribute the most to the predictive accuracy of each model.

(iv) The selected model was then retrained with the reduced input variables, and performance of the final selected models was evaluated.

5. RESULTS

In this section, we describe the comparative performance of all the statistical learning models developed (as discussed before), outline our variable selection methodology, and summarize the performance of final selected model for each sector. We also delineate our approach for estimating the seasonal long-term electricity inadequacy risks in the three different sectors.

5.1. Comparative Analysis of Model Performance for Model Selection

A summary of the performance of various models developed for each sector is provided in Table II, in terms of root mean square error (RMSE) (in-sample and out-of-sample) and mean absolute error (MAE) (in-sample and out-of-sample). The out-of-sample predictive accuracy of each of the models was calculated by performing a 30-fold random hold-out validation tests. For each model, 10% of the data was randomly held out while the model was trained with the remaining data, and the held-out sample was used to make predictions. We then calculated the RMSE and MAE for the out-of-sample predictions. This was repeated 30 times[4] (to ensure that all data were used at least once) and the averages of the RMSE and MAE are given in Table II.

From Table II, we observe that the RF-based electricity demand prediction model outperforms all other models for all the sectors in terms of goodness of fit. Also, in terms of predictive accuracy, RF is a superior model for both industrial and commercial sectors, and it comes up as the second-best model (after GAM) for the residential sector—although the difference is not statistically significant at the 5% significance level. We therefore selected the predictive model developed based on the RF algorithm as the best final model.

[4]Given that cross-validation is based on randomized subsectioning of the data into 80–20% portions, 30 times repetition is naturally a conservative measure to ensure all the values have been used at least once (Hastie, Tibshirani, & Friedman, 2008; James, Witten, Hastie, & Tibshirani, 2013).

Table III. Input Variables Selected Through Data-Driven Variable Selection Process

Predictor Set Variables	Residential	Commercial	Industrial
Monthly maximum temperature (in °F): MAX	√	√	
Mean dew point temperature (in °F): DEWP	√	√	√
Number of days with minimum temperature ≤ 32°F: DT32		√	√
Monthly mean temperature (in °F): MNTM		√	
Mean wind speed for the day (in knots): WDSP		√	
Monthly mean minimum temperature (in °F): MMNT	√	√	
Extreme minimum temperature for month (in °F): EMNT			√
Number of days with maximum temperature ≤ 32°F: DX32		√	
Extreme maximum temperature for month (in °F): EMXT	√	√	√
Monthly mean maximum temperature: MMXT		√	
Heating degree days (*balance point temperature*[a] = 65 °F): HTDD		√	
Cooling degree days (*balance point temperature* = 65 °F):CLDD	√		
Meteorological visibility (in miles): VISIB	√		
Electricity price (cents/kilowatt-hour): PRICE	√	√	√
Unemployment: UNEMPLOYMENT			√
Labor Force: LABORFORCE	√		

[a]Balance point temperature is the temperature at which the amount of electricity demanded is non-temperature-sensitive electricity load (Amato, Ruth, Kirshen, & Horwitz, 2005).

5.2. Data-Driven Variable Selection

Variable selection in a RF model is typically done via ranking the variables based on their degree of contribution to model's out-of-sample predictive accuracy (Breiman, 2001). However, as discussed earlier in Section 4.1, RF is an inherently stochastic method where the tree ensembles grown using the same set of data could be different from one another. Depending on the signal–noise ratio of the input data and the level of correlations among the independent variables, the tree structures and the resulting variable rankings may substantially change from one model to the next. To ensure a robust variable selection, we developed "forests" of the RF models and implemented full enumerations of the key predictors (and assessed the associated predictive accuracy) (Breiman, 2001; Genuer, Poggi, & Tuleau-Malot, 2010). Our variable selection algorithm involved a two-stage strategy. In the first step, multiple forests were developed and their input variables were ranked in terms of their importance (calculated based on their contribution to out-of-sample predictive accuracy) and standard deviations (Genuer et al., 2010). Variables with standard deviations below a minimum threshold (selected based on cross-validation) were then removed. Multiple nested models were then developed in a stepwise forward strategy. The smallest subset of input data that yielded the highest *out-of-sample* predictive accuracy was retained in the final model. Per Occam's razor principle, we selected the simplest model that yields the best *out-of-sample* predictive accuracy.

The list of the final key variables selected for each sector are shown in Table III. It can be observed from Table III that mean dew point temperature, extreme maximum temperature, and price of electricity (all highlighted in bold) are the key predictors across all the sectors. Also, it is noteworthy that the commercial sector's model requires the highest number of input variables to capture the climate–demand nexus.

5.3. Final Models

Once the final models were selected through a comparative analysis of in-sample fit and out-of-sample predictive accuracies of all the trained statistical models (GLM, GAM, MARS, and RF) (refer to Table II), the key predictors were identified (refer to Table III). We then retrained the models with the reduced set of key predictor variables. Table IV shows the in-sample fit and the out-of-sample predictive accuracies of both the final RF model and the "mean-only" model. The "mean-only" model uses mean of the response variable instead of a statistical model, which is a common benchmark used in statistics to identify the power of statistical models in explaining the variance of

Table IV. Comparative Analysis of Selected Models' Performance

Sectors	#	Model	R^2	In-Sample RMSE	In-Sample MAE	Out-of-Sample RMSE	Out-of-Sample MAE
Residential	1	Mean-only	NA	725.23	609.96	729.59	616.76
	2	RF	0.971	123.28	94.59	284.92	224.01
	Error reduction in selected RF compared to the "mean-only" model (%)			83%	84.5%	61%	63.7%
Commercial	1	Mean-only	NA	291.58	228.02	280.04	223.03
	2	RF	0.972	48.82	38.62	111.42	90.41
	Error reduction in selected RF compared to the "mean-only" model (%)			83.2%	83%	60.2%	59.5%
Industrial	1	Mean-only	NA	200.76	158.78	200.23	156.58
	2	RF	0.867	73.20	56.31	167.32	130.03
	Error reduction in selected RF compared to the "mean-only" model (%)			63.5%	64.5%	16.4%	17%

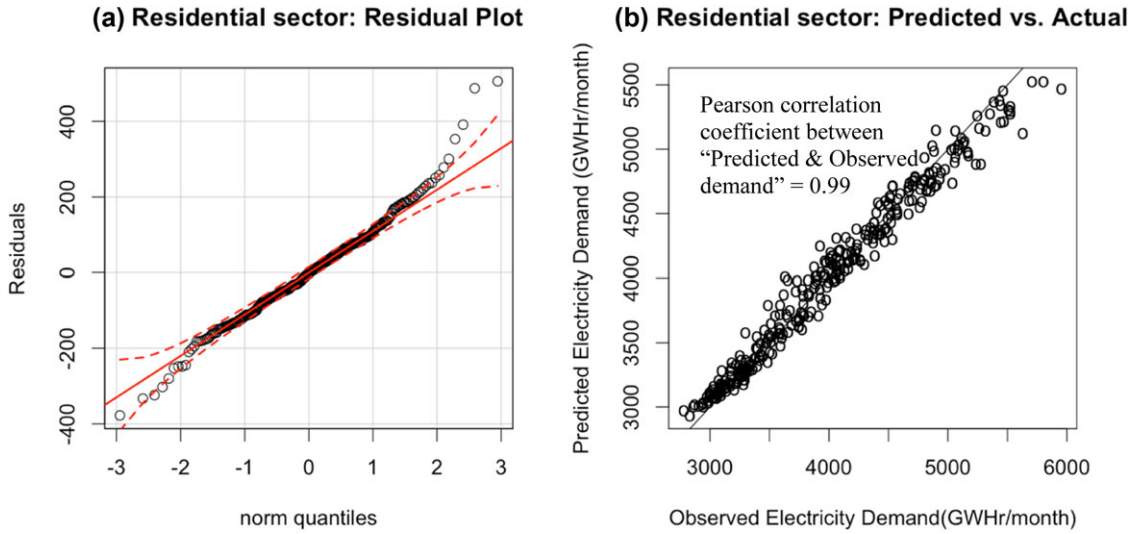

Fig. 4. Residential sector: (a) Residuals QQ plot (the red dashed lines represent 95% confidence intervals); (b) Predicted versus actual electricity consumption.

the response. It can be observed from the results in Table IV that the statistical model based on the RF algorithm outperformed the mean-only model substantially, both in terms of in-sample fit and out-of-sample predictive accuracy, in all the three sectors.

Considering the in-sample fit, we observe that the RF model yields an improvement in the range of 64–83% over the "mean-only" model in each sector. Also, the out-of-sample predictive accuracy of the model based on the RF algorithm shows an improvement in the range of 16–64% over the "mean-only" model in the three sectors.

5.4. Models' Diagnostics

Normal quantiles or QQ plots for the three sectors (Figs. 4a, 5a, and 6a for residential, commercial, and industrial sectors, respectively) show that the residuals fall along the 45-degree line of the normal quantile plot. The QQ plots and the high R^2 values indicate that the models can adequately capture the variance in the data. Moreover, the high values of Pearson correlation coefficients between the predicted and the observed values of electricity demand in the residential ($\rho = 0.99$) and commercial sectors ($\rho = 0.99$) indicate that the selected RF models adequately capture the variation in the data.

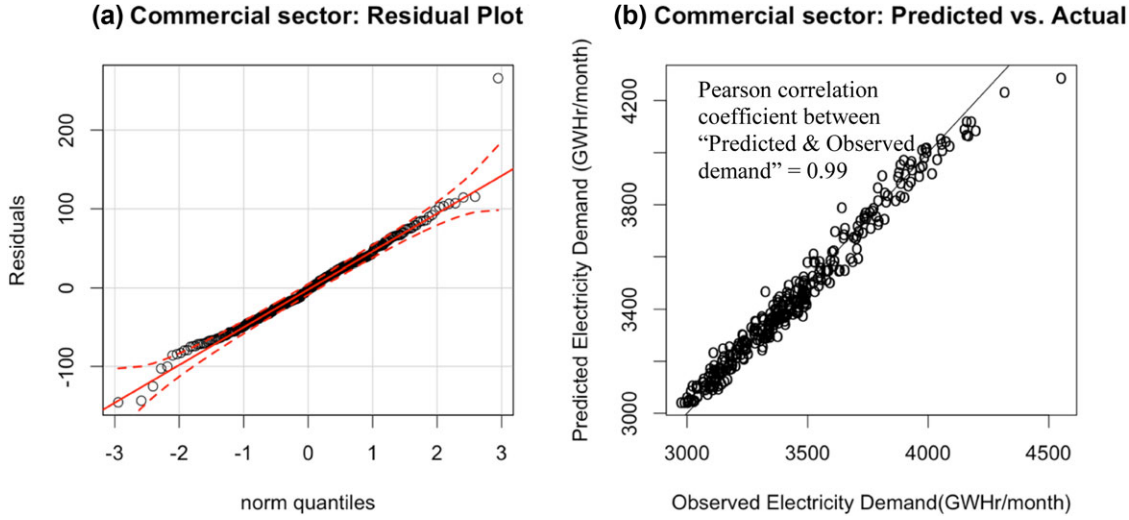

Fig. 5. Commercial sector: (a) Residual QQ plot (the red dashed lines represent 95% confidence intervals); (b) Actual versus predicted electricity consumption.

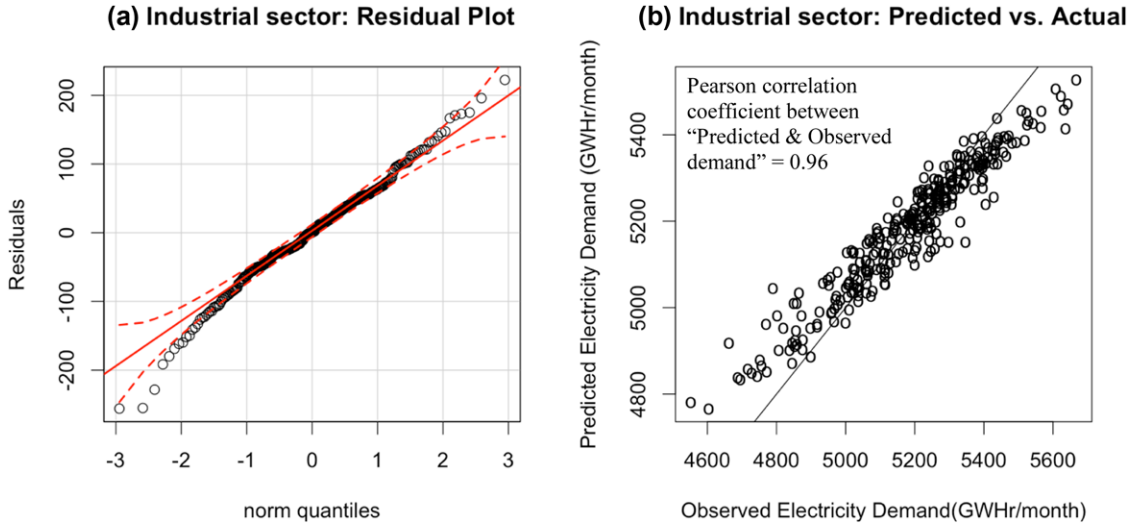

Fig. 6. Industrial sector: (a) Residual QQ plot (the red dashed lines represent 95% confidence intervals); (b) Actual versus predicted electricity consumption.

However, the observed deviations at the tails are attributable to other unobserved variables (possibly nonclimatic factors) that are required to characterize the sensitivity of demand among the energy users with more extreme profiles (e.g., substantially above or below "average" consumption levels).

On the other hand, in the industrial sector, despite the high degree of correlation ($\rho = 0.96$) between the predicted and observed values of electricity demand (Fig. 6b), the plotted points do not fall closely on the 45°line of the predicted vs. observed plot. This suggests that (an) important (nonclimate related) predictor(s) is missing from the model and, thus inducing the systematic bias. In other words, the information related to electricity demand in the industrial electricity sector is not adequately captured by the climate and weather variables alone, and there are other nonclimatic factors (e.g., the type of industry, business cycle of the industry, etc.) that significantly influence the end-use electricity demand of the industrial sector.

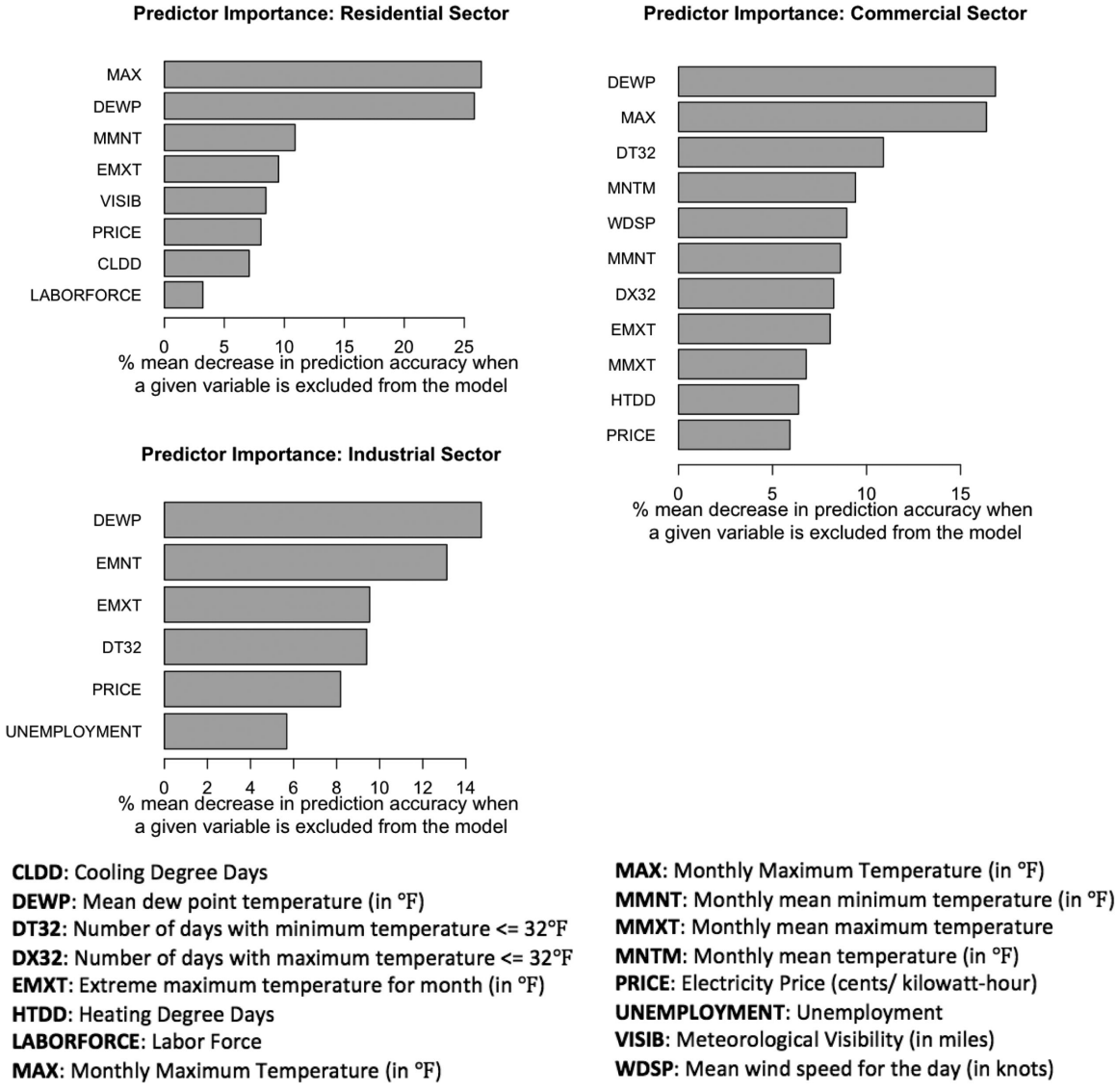

Fig. 7. Variable importance plot of the predictors.

5.5. Variable Importance and Ranking

In this section, we present the importance ranking of the predictors of electricity demand. In this article, we refer to the key climate predictors as risk factors because, under different climate scenarios, they may cause substantial deviations in the end-use electricity demand and potentially contribute to the vulnerability (electricity demand deficiency) of the electricity sector. The variable importance plots indicate that the mean dew point temperature is a key predictor across all the sectors. To understand the relationship between each of the top important predictors identified in Fig. 7 and the response, we use PDPs, as discussed in Section 5.6.

Fig. 7 shows the relative importance of the risk factors to the electricity sector in the face of climate variations. The "% mean decrease in prediction accuracy when a given variable is excluded from the model" indicates how much the predictive accuracy of the overall model is reduced—on average—if that variable is removed. The term "on average" is used here since the overall model prediction is the average of estimates across multiple trees (211 trees for the residential sector; 217 for the commercial sector; and 221 for the industrial sector).

Table V. Descriptive Statistics of Important Climate Risk Factors

Climate Risk Factors	Mean	Median	Min	Max	Std. Dev.
DEWP (in °F):	41.4	40.73	6.72	68.46	15.26
MAX (in °F):	61.75	63.15	27.08	89.44	17.29
EMNT (in °F):	26.82	27.83	−22.37	57.67	18.28

5.6. Model Inference

In this section, we discuss the key "risk factors"—i.e., the climate variables that the electricity demand is most sensitive to, —for each of the sectors. The relative influences of the risk factors on the electricity demand are illustrated using PDPs (refer to Section 4.2). It should be noted that in these plots the y-axis does not represent the actual range of end-use electricity demands as influenced by the risk factors. Instead, the y-axis in each of the plots represents the average end-use electricity demand that is influenced only by the predictor variable in the x-axis, considering all the other input variables to be constant. As shown in Fig. 7, mean dew point temperature (DEWP) and average daily maximum temperature recorded over a month (MAX) were identified as the top two climate risk factors in the residential and commercial sectors, while DEWP and extreme minimum monthly temperature (EMNT) were identified as the key risk factors in the industrial sector. Descriptive statistics of these climate risk factors are given in Table V.

Below, we discuss the partial dependencies between these risk factors and the end-use electricity demand in each of the sectors.

5.6.1. Residential Sector

Average daily maximum temperature recorded over a month (MAX) and mean dew point temperature (DEWP) are the most important "climate risk factors" in the residential sector. As observed from the PDPs in Fig. 8, both MAX and DEWP show similar "U-shaped" patterns of influence on the residential sector's electricity demand. It is noteworthy that the ranges of temperatures captured differ; with MAX capturing the higher range of temperatures compared to DEWP. Variation in DEWP signifies variation in the surface temperature combined with relative humidity. The U-shaped partial dependencies below reveal that electricity consumption is at its lowest for a MAX range of 60°F to 75°F and a DEWP range of 35°F to 50°F—the ranges that are generally considered as a comfortable zone—and, electricity consumption increases rapidly on either side of the "comfortable zones." In other words, it can be seen from Fig. 8 that during colder months, rising temperatures are associated with a decrease in heating electricity need until reaching the comfort zone after which demand rises with rising temperatures needed

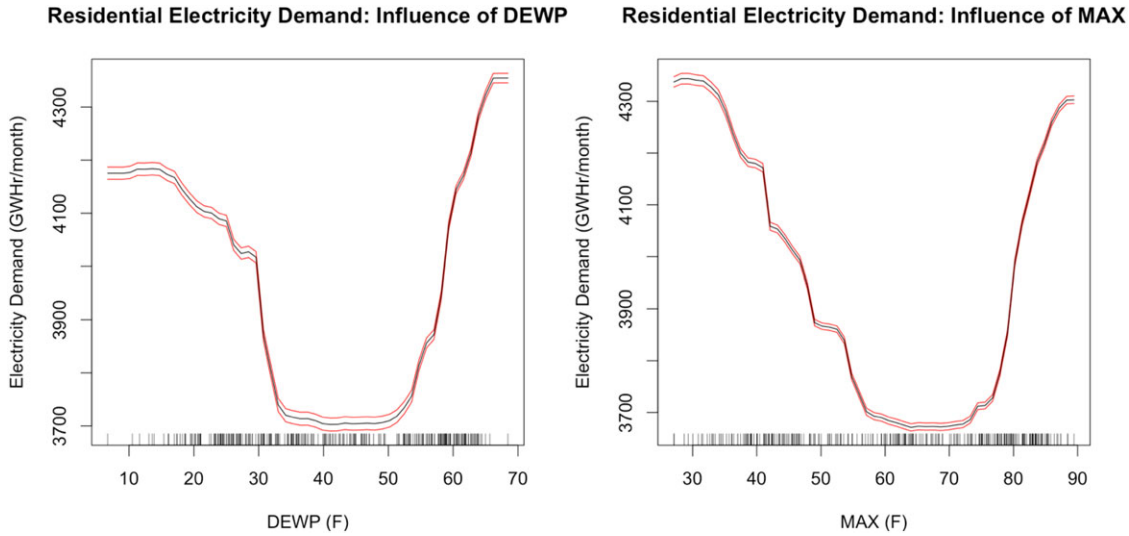

Fig. 8. Variation in DEWP and MAX influencing electricity demand in residential sector (rug lines on the x-axis indicate prevalence of data points; black curve is the average marginal effect of the predictor variable; red lines indicate the 95% confidence intervals).

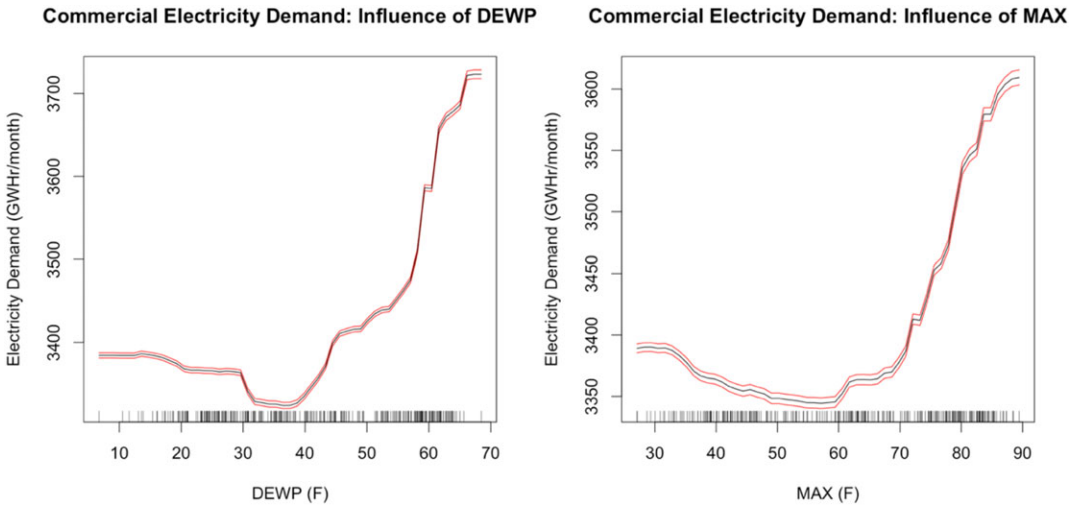

Fig. 9. Variation in DEWP and MAX influencing electricity demand in commercial sector (rug lines on the x-axis indicate prevalence of data points; black curve is the average marginal effect of the predictor variable; red lines indicate the 95% confidence intervals).

for increased space cooling. It should be noted that only 22.6% of Ohio's residents rely on electricity for space heating (as of August 2017), and with changes in the types and efficiencies of newer electric heating devices these ranges may vary even more sharply (EIA, 2017b). Fig. 8 also shows that with increase in DEWP from 50°F to 70°F, electricity demand increases by 700 GWhr/month and, when the MAX increases from 70°F to 90°F, electricity demand increases by 600 GWhr/month. This increase in electricity demand in the warmer seasons is mostly attributed to space cooling.

5.6.2. Commercial Sector

In the commercial sector, the risk of increased electricity demand is primarily due to higher temperatures during the warmer seasons—both the average monthly maximum temperature (MAX) and the mean dew point temperature (DEWP)—as the bulk of commercial building heating requirements during the colder months relies on natural gas (EIA, 2014a).

With MAX $\geq$ 60 °F and DEWP $\geq$ 40 °F, commercial electricity demand significantly rises. Fig. 9 shows with increase in DEWP from 40°F to 70°F, commercial electricity demand increases by approximately 500 GWhr/month whereas, with increase in MAX from 60°F to 90°F, commercial electricity demand increases by around 250 GWhr/month.

5.6.3. Industrial Sector

The industrial sector shows lower climate sensitivity compared to the residential or commercial sectors. Like the other two sectors, DEWP is identified as the most important climate variable influencing the industrial sector's electricity demand. The extreme minimum temperature recorded in a month (EMNT) was also identified as a top predictor in this sector. Fig. 10 shows that with increase in DEWP from 10°F to 70°F, the industrial electricity demand increases by 100 GWhr/month.

Comparing the marginal influences of DEWP on electricity demand of the three sectors, we observed that the residential sector is most sensitive to temperature rise (and potentially more vulnerable under certain climate change scenarios), followed by the commercial and industrial sectors, respectively.

6. SENSITIVITY OF DEMAND UNDER CLIMATE PERTURBATIONS

In this section, we present an approach of analyzing the variations in end-use electricity demand patterns under climate perturbations, to assess the end-use electricity demand sensitivity to various climate and weather variables. Generally, sensitivity to climate change is either implemented using specific climate scenarios (e.g., IPCC scenarios), or leveraging the more traditional method of statistical sensitivity analysis (Sailor, 2001). Due to large degrees of uncertainties associated with the projected climate change

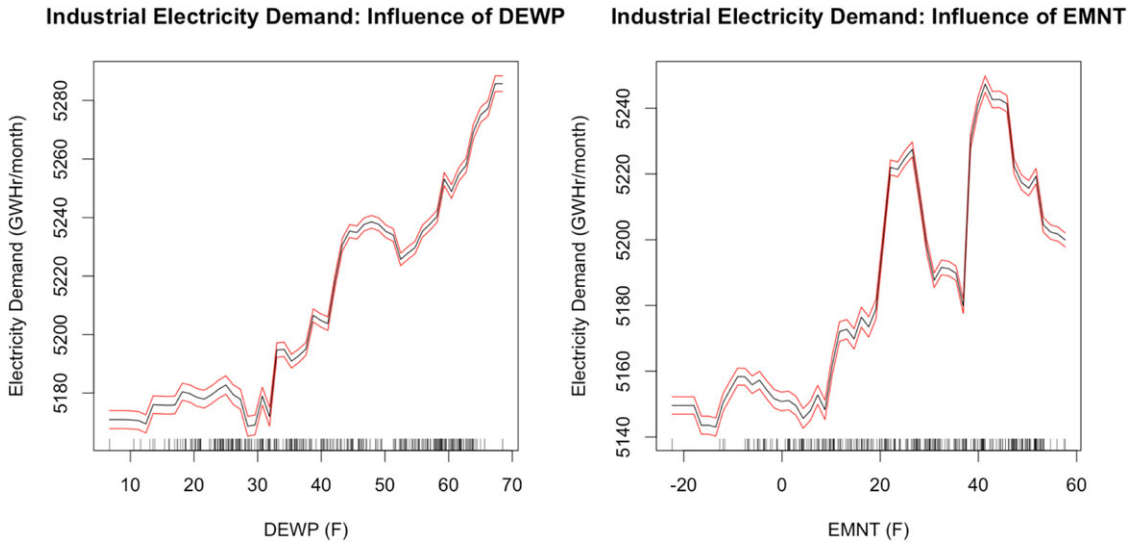

Fig. 10. Variation in DEWP and EMNT influencing electricity demand in industrial sector (rug lines on the x-axis indicate prevalence of data points; black curve is the average marginal effect of the predictor variable; red lines indicate the 95% confidence intervals).

scenarios using general circulation models (GCM), and also uncertainty in downscaling the climate scenarios to state level, we limited our analysis to statistical perturbation. Leveraging a statistical-based simulation approach, we projected the future climate change scenarios. More specifically, our analysis reveals that if, at a given point in time, the climate parameters are deviated by 0.5/1 or 2 standard deviations, then the demand will vary by X% compared to the "as-is" or "baseline" scenario. We used the projections for 2033 since that was the farthest future-cast accessible at this point in time. Based on our prior conversations with experts in the field, we gathered that in light of large deviations across the many different climate change models (particularly in the Midwest), a 2σ (standard deviation) change in temperature over the next two decades is extreme, but is not unimaginable. This proposed approach can also be easily extended to using different IPCC climate scenarios.

For the sake of brevity in this article, we only focus on perturbing the key common climate risk factor—namely, the mean dew point temperature (DEWP)—across all the sectors. However, the method can be applied to all other key predictors as well. It is to be noted that in this article, we only present a framework to perturb one of the input predictors, i.e., DEWP, that was found to be highly important across all the three sectors. However, since there are correlations between the input climate and weather covariates, implementing a multivariate sensitivity analysis is important, but it is beyond the scope of this article. Unlike some previous approaches of perturbing the mean values of climate variables deterministically (Sailor, 2001), we perturbed the average values of the climate variables probabilistically by increasing the mean by 0.5, 1, and 2 standard deviations (σ). More specifically, we considered the following scenarios of DEWP perturbations:

(1) **Baseline**: base case, with no perturbation (BASELINE)
(2) **Scenario-1**: monthly DEWP is increased by 0.5σ (MINOR) indicating a minor shift in climate
(3) **Scenario-2**: monthly DEWP is increased by 1σ (MODERATE) indicating a moderate climatic change
(4) **Scenario-3**: monthly DEWP is increased by 2σ (EXTREME) indicating an extreme climatic change

For each of the above-mentioned scenarios, simulated data sets are generated with the perturbed climate variable of interest (here, DEWP). The sectoral electricity demand under such scenarios is then predicted using the developed predictive models for the respective sectors.

Figs. 11–13 depict the predicted monthly electricity demand increase for the residential, commercial,

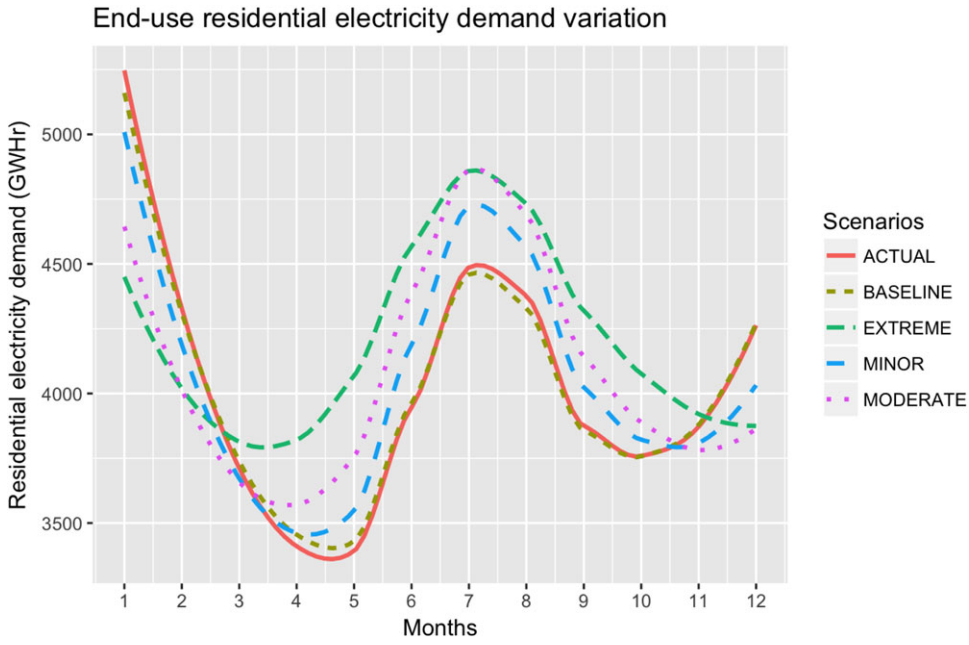

Fig. 11. Residential sector: Electricity demand under DEWP perturbation scenarios.

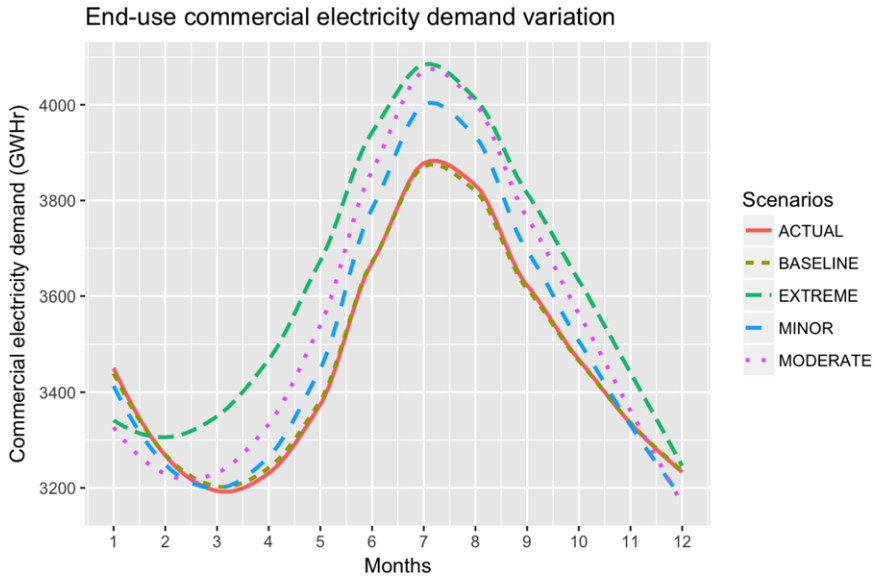

Fig. 12. Commercial sector: Electricity demand under DEWP perturbation scenarios.

and industrial sectors under four different scenarios mentioned above. We also show the "ACTUAL" scenario, representing the observed monthly electricity demand using historical data. This helps to compare our estimated electricity demand under various climate scenarios with the historical data. Moreover, it can be also used to validate the baseline predictions against historical data. As can be seen from Figs. 11–13, our models' estimates under the baseline scenario and the historical data closely match for all sectors.

For the residential sector, it is observed that under different perturbed climate scenarios, electricity demand is projected to decrease during the winter months (from November to February). The demand again significantly increases during the warmer

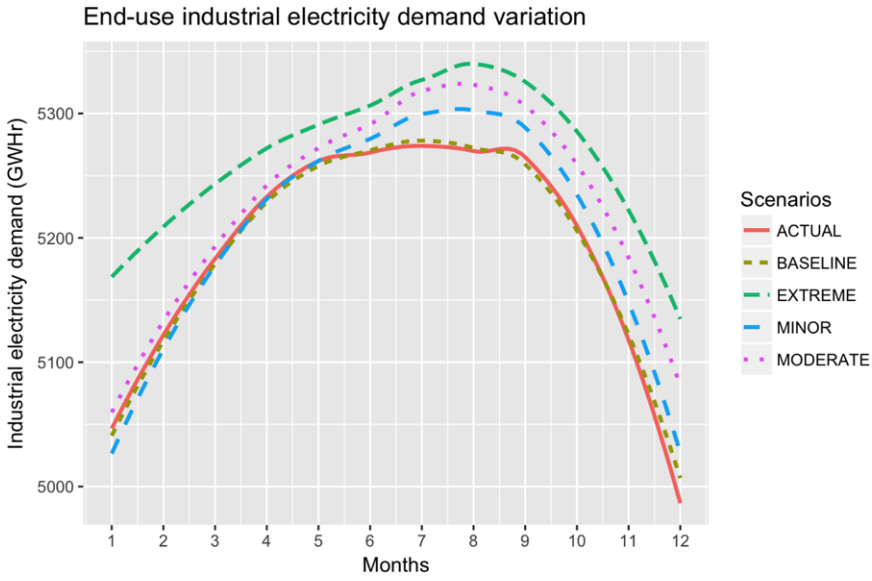

Fig. 13. Industrial sector: Electricity demand under DEWP perturbation scenarios.

(spring/summer/fall) months (March to October), as compared to the existing climate conditions. The reduction in the winter electricity demand is mostly attributed to reduced space heating requirements because of higher mean dew point temperatures. Similarly, higher temperatures in the warmer months increase the electricity demand for cooling. The peak demand in summer occurs during the month of July, and it increases by around 250 GWHr under minor climate change to around 400 GWHr under extreme climatic change conditions (Fig. 11).

In the commercial sector, the patterns of electricity demand change under various climate scenarios are like that of the residential sector. The only difference is lower variations are observed in electricity demand during the winter months under climate change situations. Under minor and moderate climatic change, the electricity demand shows a slight decrease during the months of January and February, but shows a steady increase during those months under extreme climate perturbations. The commercial demand increases steadily as the perturbed climate shifts from minor to extreme; and reaches a peak during the month of July, and then steadily decreases. The peak electricity demand increases by about 150 GWHr for minor climatic change to about 400 GWHr for extreme climatic change as compared to the baseline in the commercial sector (Fig. 12).

In the industrial sector, there is not much variation in the monthly electricity demand under the climate perturbation scenarios. Unlike the residential sector, electricity demand increases both during the winter and the summer months, reaching peak demand in the month of August. However, it is observed from Fig. 13 that the average peak demand ranges from 5,250 GWHr/month (under minor climate change condition) to 5,350 GWHr/month (under to extreme climate change condition), which further highlights that industrial electricity demand is much less sensitive to climate change as compared to the residential and commercial sectors.

7. COMMUNICATING "RISK MAPS" TO DECISIONMAKERS

To communicate the results of inadequacy risks under various scenarios more effectively with stakeholders and decisionmakers, we propose using heatmaps. Heat maps are powerful visualization tools for communicating statistical information. The heat maps plotted in this section represent the relative risks in monthly electricity demand increase for each of the sectors under minor, moderate, and extreme climate perturbations.

In the context of the residential sector (Fig. 14), it is observed that under the minor climatic change scenario (i.e., the first row from the bottom on the heat map associated with 0.5σ increase in the monthly value of DEWP), the probability of having increased electricity demand is higher during the summer months (June–August). Under moderate

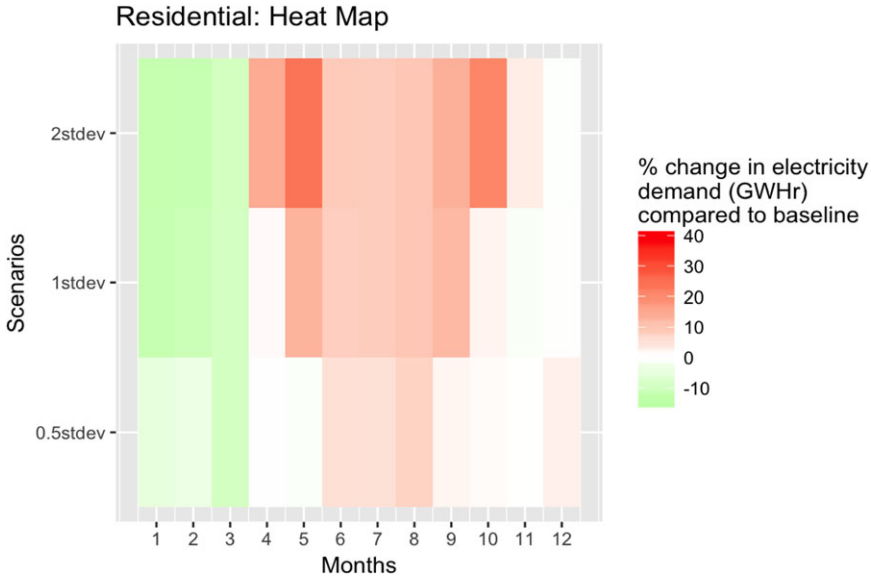

Fig. 14. Residential sector: Percentage of climate-induced change in monthly electricity demand under DEWP perturbation scenarios (green color shades indicate decrease in electricity demand, white color indicates no change in electricity demand, and shades of red indicate increase in electricity demand under various climate perturbation scenarios compared to the no climate change [baseline] scenario).

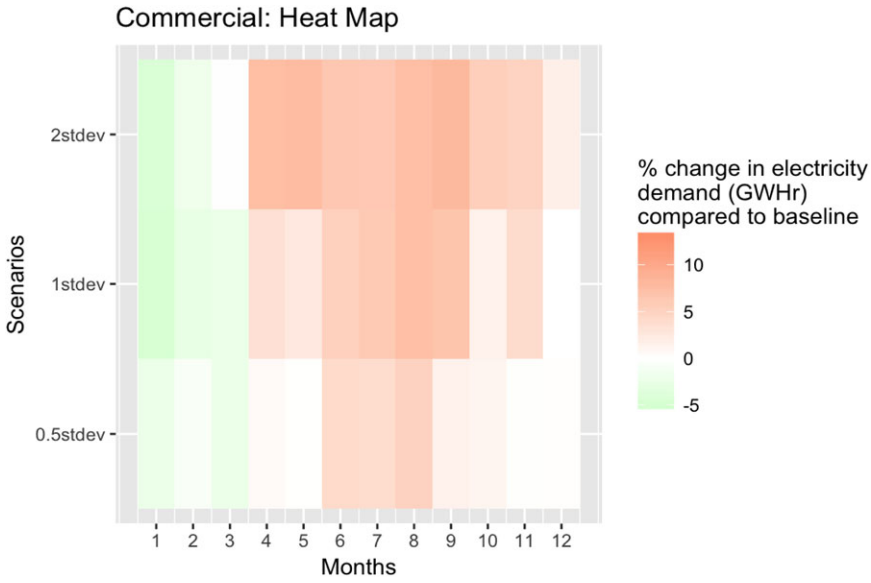

Fig. 15. Commercial sector: Percentage of climate-induced change in monthly electricity demand under DEWP perturbation scenarios (green color shades indicate decrease in electricity demand, white color indicates no change in electricity demand, and shades of red indicate increase in electricity demand under various climate perturbation scenarios compared to the no climate change [baseline] scenario).

and extreme climatic change scenarios, the range of months for which higher electricity demands are observed is wider (April–October) as compared to the minor climatic change scenario. It can be observed that, compared to the baseline, i.e., no climate change scenario, the electricity demand might increase by more than 10–20% of the mean consumption during the summer months under moderate climate change, and by more than 20–40% of the mean consumption under the extreme climatic change scenario. These likely considerable shifts in electricity demand under climate contingencies could be alarming, as the

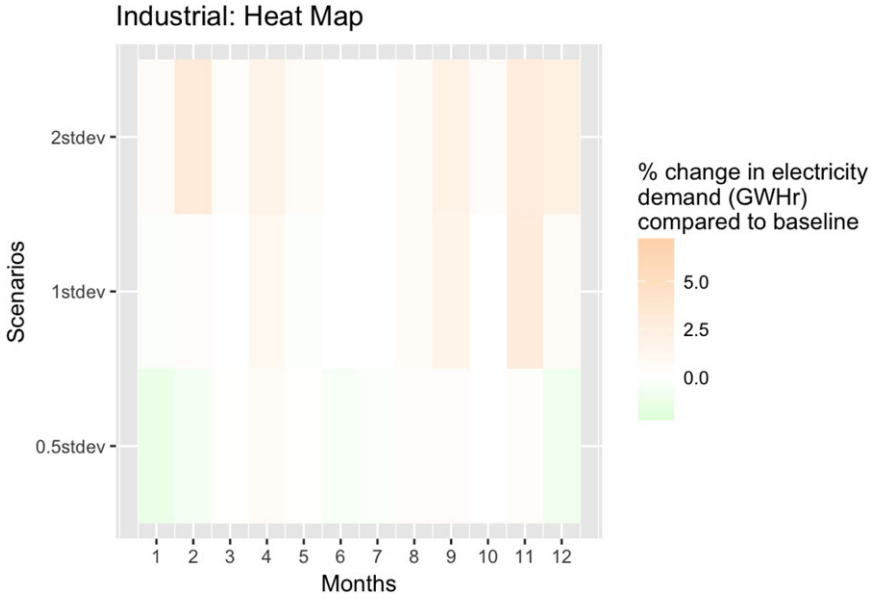

Fig. 16. Industrial sector: Percentage of climate-induced change in monthly electricity demand under DEWP perturbation scenarios (green color shades indicate decrease in electricity demand, white color indicates no change in electricity demand, and shades of red indicate increase in electricity demand under various climate perturbation scenarios compared to the no climate change [baseline] scenario).

projected residential electricity demand by officials is much more modest. According to a recent report by the Public Utility Commission of Ohio (PUCO), the residential sector's *annual electricity demand* is forecasted to increase from 52.2 million MWH in 2013 to: (1) 52.9 million MWH in 2021, i.e., 1.34% increase in electricity demand by 2021; (2) 53.2 million MWh in 2024, i.e., 1.9% increase by 2024; and (3) 54.1 million MWh in 2033, i.e., 3.64% hike by 2033 (PUCO, 2015). These small projected margins of demand increase may signal lower than needed investment in capacity expansion, which is likely to render this sector vulnerable to "unanticipated" demand hikes under a warmer climate.

A similar pattern of electricity demand increase is observed in the commercial sector (Fig. 15). This sector is likely to see a peak in demand increase in the range of around 0–7% of the mean consumption to 5–14% of mean consumption per month during March to December. It can be observed that compared to the residential sector, the commercial sector is insensitive to climate change and variations. The PUCO projected the *annual commercial electricity demand* to increase from 46.8 million MWh in 2013 to: (1) 47.2 million MWh in 2021, i.e., 0.85% increase in electricity demand by 2021; (2) 47.3 million MWh in 2024, i.e., 1.1% increase by 2024; and (3) 48.3 million MWh in 2033, i.e., 3.2% hike by 2033 (PUCO, 2015). Again, projected demand increases are likely underestimated, and potentially do not account for climate sensitivity of demand in this sector.

Unlike residential and commercial sectors, the industrial sector is significantly less influenced by the perturbed climate scenarios and the demand is likely to increase in the colder months as opposed to the warmer months in the other two sectors (Fig. 16).

8. CONCLUSION

The electricity sector underlies the economic prosperity of every society and it is important to ensure its reliability under various plausible contingencies. Adequacy planning in this sector commands knowledge of demand patterns and their evolution under various likely stressors such as shifts in population, socio-techno-economic, and climatic change. In this article, we focused on identifying the climate sensitivity of load and proposed a place-based, data-driven framework to identify climatic risk factors in residential, commercial, and industrial sectors. While projecting the possible shifts in customer behavior in response to changes in policy, technology, and socioeconomic factors is critical for adequacy planning, it was outside the scope of analysis presented in this article. Our results indicated that mean dew point temperature and average daily maximum

temperature are the key predictors of the climate-sensitive portion of the load in the residential and commercial sectors. The residential sector was found to be most sensitive to climate variations and change, followed by the commercial sector. The industrial load revealed significantly less climate sensitivity compared to the residential and commercial loads, with mean dew point temperature and extreme minimum monthly temperature identified as the key climate risk factors.

We used statistical sensitivity analyses to simulate the evolution of electricity demand in different sectors under different perturbed climate scenarios. Our results indicated that, under all scenarios, the residential and commercial electricity demand will likely decrease during winter and increase during the summer seasons. However, the industrial demand will likely increase in the colder months—as opposed to the other two sectors that witness demand increase during the warmer months. A comparison of our estimates with the projections of the PUCO revealed that the climate sensitivity of demand is currently underestimated. Underestimating climate-driven demand growth will likely lead to supply inadequacy risks if the continued deviation from average temperatures persist in this region. Our proposed heat maps can be used to better communicate the scenario-based climate sensitivity of demand to decisionmakers and better inform them on the climate risks in various sectors.

ACKNOWLEDGMENTS

The authors would like to thank the Purdue Climate Change Research Center (PCCRC) and National Science Foundation (NSF SEES #1555582 and NSF #1728209) for providing support and funding for this project. The authors would like to thank Ruixin Wang for assistance in data collection.

APPENDIX

In this section, we include the methodological backgrounds on GLM, GAM, and MARS models.

Appendix A: Generalized Linear Model (GLM)

Nelder and Wedderburn introduced GLM in early 1970s (Nelder & Wedderburn, 1972). A GLM is an extension of the linear regression as it relaxes the normality assumption of the OLS estimation method. In a GLM formulation, the dependent variable Y belongs to an exponential family and can be mathematically defined as follows:

$$\mathbf{Y} \sim f_{Y_i}(y_i), \tag{1}$$

$$f_{Y_i}(y_i) = \exp\left\{\frac{y_i\theta_i - b(\theta_i)}{a(\phi)} + c(y_i, \phi)\right\}, \tag{2}$$

here, $f_{Y_i}(y_i)$ is the probability density function of Y; θ_i is called the natural parameter and is a function of $x_{i1}, x_{i2}, \ldots, x_{ip}$ that involves unknown parameters; ϕ is the scale parameter that is constant for all observations, i; and $x_{i1}, x_{i2}, \ldots, x_{ip}$ is a set of p independent variables on which the response variable is dependent.

The linear combination of the predictor variables, referred to as the systemic component, is shown in Equation (3).

$$\eta = \beta_0 + \sum_{j=1}^{p} \beta_j x_{ij} \tag{3}$$

This systemic component, η, is linked to the response through a link function $g(.)$ to render the final model (Guikema & Coffelt, 2008).

The advantage of GLM is that it is easy to fit and interpret and has been widely used to model various types of data. However, due to its rigid parametric assumptions, it often yields inferior predictions compared to semi-parametric and nonparametric models and is not suitable for highly nonlinear and high dimensional data.

Appendix B: Generalized Additive Model

GAM is a semi-parametric method that relaxes the linearity assumption of GLM and allows for local nonlinearities (Hastie & Tibshirani, 1990; Hastie & Tibshirani, 1986). A GAM assumes that the response variable, $\mathbf{Y}$, follows a distribution with mean $\mu = E[\mathbf{Y}|x_1, x_2, \ldots..x_p]$ that is linked to the predictors $x_1, x_2, \ldots x_p$ via the link function $g(.)$ such that $g(\mu_i) = \alpha + \sum_{j=1}^{p} f_j(x_j)$; here, each f_j is a smoothing function of a specified class of functions estimated nonparametrically, like regression splines or tensor product splines. The significant advantage of GAM is that it substantially improves the model performance—especially over parametric models such as OLS or GLM—by better capturing the complex structure of the data (Guikema & Coffelt, 2008). However, in the absence of careful cross-validation, it is prone to overfitting.

Appendix C: Multivariate Adaptive Regression Splines

MARS is a semi-parametric adaptive procedure for regression that is well suited and efficient for high-dimensional data spaces (Friedman, 1991). It can be described as a generalized stepwise linear regression. A MARS model consists of sum-of-splines that allow the response variable to vary nonlinearly with the input variables as represented by $f(\mathbf{X}) = \beta_0 + \sum_{m=1}^{M} \beta_m h_m(\mathbf{X})$. Here, each $h_m(x)$ represents the linear splines, β_0 represents the intercept, and β_m represents the vector of the coefficients. β_m coefficients are estimated by minimizing the sum of square errors. The advantage of MARS is that it can allow both nonlinear and interdependent explanatory effects and thus can have significantly high predictive power. However, similar to GAM, it can be prone to overfitting if the model parameters are not carefully selected based on rigorous cross-validation (Guikema & Coffelt, 2008).

REFERENCES

Amato, A. D., Ruth, M., Kirshen, P., & Horwitz, J. (2005). Regional energy demand responses to climate change: Methodology and application to the commonwealth of Massachusetts. *Climatic Change*, *71*(1), 175–201. https://doi.org/10.1007/s10584-005-5931-2

ASCE. (2017). Infrastructure Report Card: A Comprehensive Assessment of America's Infrastructure. Retrieved from https://www.infrastructurereportcard.org (accessed on September 06, 2018).

Birkmann, J. (2006). Measuring vulnerability to promote disaster-resilient societies: Conceptual frameworks and definitions. *Measuring Vulnerability to Natural Hazards: Towards Disaster Resilient Societies*, *1*, 9–54.

Breiman, L. (2001). Random forests. *Machine Learning*, *45*(1), 5–32. https://doi.org/10.1023/A:1010933404324

Brown, M. A., Cox, M., Staver, B., & Baer, P. (2014). Climate change and energy demand in buildings. In *2014 ACEEE summer study on energy efficiency in buildings* (3–26–23–38). Retrieved from https://aceee.org/files/proceedings/2014/data/index.htm.

Chandramowli, S. N., & Felder, F. A. (2014). Impact of climate change on electricity systems and markets—A review of models and forecasts. *Sustainable Energy Technologies and Assessments*, *5*, 62–74.

Crowley, C., & Joutz, F. L. (2005). *Weather effects on electricity loads: Modeling and forecasting*. Retrieved from https://www.ce.jhu.edu/epastar2000/epawebsrc/joutz/Final Report EPA Weather Effects on Electricity Loads.pdf. (accessed on September 05, 2018).

Davis, M., & Clemmer, S. (2014). *Power failure: How climate change puts our electricity at risk and what we can do*. Retrieved from https://www.ucsusa.org/powerfailure. (accessed on September 06, 2018).

DOE. (2013). *U.S. energy sector vulnerabilities to climate change and extreme weather*. Retrieved from https://www.energy.gov/sites/prod/files/2013/07/f2/20130710-Energy-Sector-Vulnerabilities-Report.pdf (accessed on September 06, 2018).

DOE. (2015). *Climate change and the U.S. energy sector: Regional vulnerabilities and resilience solutions*. Retrieved from https://www.energy.gov/sites/prod/files/2015/10/f27/Regional_Climate_Vulnerabilities_and_Resilience_Solutions_0.pdf (accessed September 06, 2018).

DOE. (2016). *Climate change and the electricity sector: Guide for climate change resilience planning*. Retrieved from https://www.energy.gov/sites/prod/files/2016/07/f33/Climate%20Change%20and%20the%20Electricity%20Sector%20Guide%20for%20Assessing%20Vulnerabilities%20and%20Developing%20Resilience%20Solutions%20to%20Sea%20Level%20Rise%20July%202016.pdf (accessed September 06, 2018).

EIA. (2014a). *Natural gas is the dominant heating fuel in colder parts of the country*. Retrieved from https://www.eia.gov/todayinenergy/detail.php?id=18811 (accessed on September 06, 2018).

EIA. (2014b). *The Electricity Market Module of the National Energy Modeling System: Model documentation 2014*. Washington, DC. Retrieved from https://www.eia.gov/outlooks/aeo/nems/documentation/electricity/pdf/m068(2014).pdf (accessed on September 06, 2018).

EIA. (2017a). *Form EIA-861M (formerly EIA-826) detailed data*. Retrieved from https://www.eia.gov/electricity/data/eia861m/ (accessed on September 06, 2018).

EIA. (2017b). *Ohio state energy profile*. Retrieved from https://www.eia.gov/state/print.php?sid=OH (accessed on September 06, 2018).

Friedman, J. H. (1991). Multivariate adaptive regression splines. *Annals of Statistics*, *19*(1), 1–67. Retrieved from https://www.jstor.org/stable/2241837.

Gallopín, G. C. (2006). Linkages between vulnerability, resilience, and adaptive capacity. *Global Environmental Change*, *16*(3), 293–303. https://doi.org/10.1016/j.gloenvcha.2006.2.004

Genuer, R., Poggi, J.-M., & Tuleau-Malot, C. (2010). Variable selection using random forests. *Pattern Recognition Letters*, *31*(14), 2225–2236. https://doi.org/10.1016/j.patrec.2010.03.014

Guikema, S. D., & Coffelt, J. P. (2008). Modeling count data in risk analysis and reliability engineering. In *Handbook of performability engineering* (pp. 579–594). London: Springer. https://doi.org/10.1007/978-1-84800-131-2

Hastie, T., & Tibshirani, R. (1986). Generalized additive models. *Statistical Science*, *1*(3), 297–310. Retrieved from https://www.jstor.org/stable/2245459.

Hastie, T. J., & Tibshirani, R. J. (1990). *Generalized additive models* (1st ed.). Chapman and Hall/CRC Press.

Hastie, T. J., Tibshirani, R. J., & Friedman, J. H. (2003). *The elements of statistical learning: Data mining, inference and prediction* (2nd ed.). Springer Series in Statistics. Retrieved from https://web.stanford.edu/~hastie/Papers/ESLII.pdf (accessed on September 06, 2018).

Hastie, T., Tibshirani, R., & Friedman, J. H. (2008). *The elements of statistical learning* (2nd ed.). Springer Series in Statistics.

Hines, P., Apt, J., & Talukdar, S. (2009). Large blackouts in North America: Historical trends and policy implications. *Energy Policy*, *37*(12), 5249–5259. https://doi.org/10.1016/j.enpol.2009.07.049

Hintze, J. L., & Nelson, R. D. (1998). Violin plots: A box plot-density trace synergism. *American Statistician*, *52*(2), 181–184.

Hirst, E. (1992). Price and cost impacts of utility DSM programs. *Energy Journal*, 75–90.

IEA. (2015). *Energy and climate change*. Retrieved from https://www.iea.org/publications/freepublications/publication/WEO2015SpecialReportonEnergyandClimateChange.pdf (accessed on September 06, 2018).

James, G., Witten, D., Hastie, T., & Tibshirani, R. (2013). *An introduction to statistical learning—With applications in R*. In G. F. S. Casella & I. Olkin (Eds.). New York: Springer.

Kapelner, A., & Bleich, J. (2013). Bartmachine: Machine learning with Bayesian additive regression trees. Retrieved from

https://arxiv.org/pdf/1312.2171.pdf (accessed on September 06, 2018).

Keogh, M., & Cody, C. (2013). *Resilience in regulated utilities*. Retrieved from https://pubs.naruc.org/pub/536F07E4-2354-D714-5153-7A80198A436D (accessed on September 06, 2018).

Li, W. (2014). *Risk assessment of power systems: Models, methods, and applications*. (2nd ed.). Wiley-IEEE Press.

Loulou, R., Goldstein, G., & Noble, K. (2004). Documentation for the MARKAL Family of Models. Retrieved from https://iea-etsap.org/MrklDoc-I_StdMARKAL.pdf (accessed on September 06, 2018).

Mideksa, T. K., & Kallbekken, S. (2010). The impact of climate change on the electricity market: A review. *Energy Policy*, *38*(7), 3579–3585.

Miller, N. L., Jin, J., Hayhoe, K., & Auffhammer, M. (2007). Climate change, extreme heat, and electricity demand in California: CEC-500-2007-023.

Mirasgedis, S., Sarafidis, Y., Georgopoulou, E., Kotroni, V., Lagouvardos, K., & Lalas, D. P. (2007). Modeling framework for estimating impacts of climate change on electricity demand at regional level: Case of Greece. *Energy Conversion and Management*, *48*(5), 1737–1750. https://doi.org/10.1016/j.enconman.2006.10.022

Mukherjee, S. (2017). *Towards a resilient grid: A risk-based decision analysis incorporating the impacts of severe weather-induced power outages*. Purdue University.

Mukherjee, S., & Hastak, M. (2016). Public utility commissions to foster resilience investment in power grid infrastructure. *Procedia - Social and Behavioral Sciences*, *218*, 5–12. https://doi.org/10.1016/j.sbspro.2016.04.005

Mukherjee, S., & Hastak, M. (2017). Optimal selection of transmission line rehabilitation strategies to minimize power transmission costs. In *Project Management Research & Academic Conference 2017*. Indian Institute of Technology, Delhi.

Mukherjee, S., & Nateghi, R. (2017). Climate sensitivity of end-use electricity consumption in the built environment: An application to the state of Florida, United States. *Energy*, *128*, 688–700. https://doi.org/10.1016/j.energy.2017.04.034

Mukherjee, S., & Nateghi, R. (2018). Estimating climate-demand nexus to support long-term adequacy planning in the energy sector. In *2017 IEEE Power & Energy Society General Meeting* (pp. 1–5). IEEE Xplore. https://doi.org/10.1109/PESGM.2017.8274648

Mukherjee, S., Nateghi, R., & Hastak, M. (2018). A multi-hazard approach to assess severe weather-induced major power outage risks in the U.S. *Reliability Engineering & System Safety*, *175*(July), 283–305. https://doi.org/10.1016/j.ress.2018.03.015

Mukherjee, S., Vineeth, C.R., & Nateghi, R. (2018). Evaluating regional climate-electricity demand nexus: A composite Bayesian predictive framework. *Applied Energy* (under review).

Nateghi, R., Guikema, S. D., Wu, Y. G., & Bruss, C. B. (2016). Critical assessment of the foundations of power transmission and distribution reliability metrics and standards. *Risk Analysis*, *36*(1), 4–15.

Nateghi, R., & Mukherjee, S. (2017). A Multi-paradigm framework to assess the impacts of climate change on end-use energy demand. *PloS One*, *12*(11), e0188033. https://doi.org/10.1371/journal.pone.0188033

Nelder, J. A., & Wedderburn, R. W. M. (1972). Generalized linear models. *Journal of the Royal Statistical Society. Series A (General)*, *135*(3), 370–384. Retrieved from https://www.jstor.org/stable/2344614.

NERC. (2007). *Definition of "adequate level of reliability*." Retrieved from https://www.nerc.com/docs/pc/Definition-of-ALR-approved-at-Dec-07-OC-PC-mtgs.pdf (accessed on September 06, 2018).

NOAA. (2016a). National Overview—June 2016. Accessed December 26, 2016, Retrieved from https://www.ncdc.noaa.gov/sotc/national/201606 (accessed on September 06, 2018).

NOAA. (2016b). *National temperature and precipitation maps*. Retrieved from https://www.ncdc.noaa.gov/temp-and-precip/us-maps/6/201606#us-maps-select (accessed on September 06, 2018).

NYISO. (2016). *Power trends 2016: The changing energy landscape*. Retrieved from https://www.nyiso.com/public/webdocs/media_room/publications_presentations/Power_Trends/Power_Trends/2016-power-trends-FINAL-070516.pdf (accessed on September 06, 2018).

Pielke, R. A. S., Davey, C., & Morgan, J. (2004). Assessing "global warming" with surface heat content. *Eos Transactions American Geophysical Union*, *85*(21), 210–211. https://doi.org/10.1029/2004EO210004

PJM Interconnection. (2016). *Load forecasting model whitepaper*. Retrieved from https://www.pjm.com/~/media/library/reports-notices/load-forecast/2016-load-forecast-whitepaper.ashx (accessed on September 06, 2018).

PUCO. (2015). *Ohio long term forecast of energy requirements*. Retrieved from https://www.puco.ohio.gov/industry-information/statistical-reports/ohio-long-term-energy-forecast/ohio-ltfr-2017-2036/ (accessed on September 08, 2018).

Ruth, M., & Lin, A.-C. (2006). Regional energy demand and adaptations to climate change: Methodology and application to the state of Maryland, USA. *Energy Policy*, *34*(17), 2820–2833. https://doi.org/10.1016/j.enpol.2005.04.016

Sailor, D. J. (2001). Relating residential and commercial sector electricity loads to climate—Evaluating state level sensitivities and vulnerabilities. *Energy*, *26*(7), 645–657.

Sailor, D. J., & Muñoz, J. R. (1997). Sensitivity of electricity and natural gas consumption to climate in the U.S.A.—Methodology and results for eight states. *Energy*, *22*(10), 987–998.

Stockton, P. (2014). *Resilience for black sky days*. Retrieved from https://www.sonecon.com/docs/studies/Resilience_for_Black_Sky_Days_Stockton_Sonecon_FINAL_ONLINE_Feb5.pdf (accessed September 06, 2018).

Sullivan, P., Colman, J., & Kalendra, E. (2015). *Predicting the response of electricity load to climate change*. Retrieved from https://www.nrel.gov/docs/fy15osti/64297.pdf (accessed on September 06, 2018).

USDL. (2016). *Bureau of Labor Statistics: Data tools*. Retrieved from https://www.bls.gov/data/ (accessed September 06, 2018).